System modelling, stability analysis and motion control using a novel technique

Imran S. Sarwar

Abstract— The ability to identify and follow a moving object is not only important for human activities, but it is also critical necessity in the use of robots for automation and manufacturing, security applications, and for life sciences. This can be achieved by using the two degree of freedom (2-DOF) robotic system with a camera. For this purpose, dynamical model of pan and tilt mechanisms were determined by using Newton-Euler equation and bond graph model. The stability analysis of dynamical models is performed before designing the motion controllers for the 2-DOF robotic system. To perform the analysis and simulation, all the parameters involved in the system dynamics were identified. The objective of this research work is to derive motion controllers for the pan and tilt mechanisms based on dynamical model and model the controller using bond graph modelling technique this adds the new dimension in modelling. These controllers make possible for camera to point in a desired direction within allowable specifications.

Index Terms— Application, bond graph modelling, control system, lead compensator, robotic system, stability analysis, system modelling, simulation.

1 Introduction

THE schematic of the tilt mechanism has been shown in fig. 1 along with computer aided design (CAD) of tilt mechanism. The tilt mechanism is supporting and orienting the device (camera) in a desired direction. The tilt mechanism is rotatable about a tilt axis supported on the pan mechanism. The tilt motor drives the tilt mechanism. There is a drive pulley on the shaft of the motor. Through the mechanism of pulleys and V-belt, the torque is transferred to the camera platform. This mechanism has one revolute joint (R).

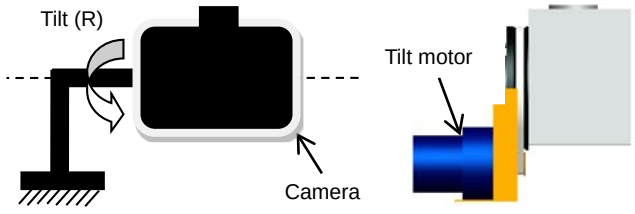

Fig. 1. (a) Schematics and (b) CAD of the tilt mechanism

The schematic of the pan mechanism has one degree of freedom as shown in fig. 2(a). The CAD of pan mechanism is presented in fig. 2(b). The pan mechanism is supporting and orienting the tilt mechanism in the desired direction. The pan mechanism is rotatable about a pan axis. The base plate has rigid joint with vertical supports. It can be fixed on any vehicle such as an aircraft. The pan motor drives the pan mechanism. Similarly, in fig. 2(b), a drive pulley is fixed on the shaft of the motor and another pulley is fixed with the supporting plate. Through this mechanism of pulleys and V-belt, the torque is transferred to the structure as shown in fig. 2.

• *Imran S. Sarwar is working as a lecturer in the Air university, Pakistan PH-00923419507775; email: imransarwar@mail.au.edu.pk.*

The bond graph model (BGM) of the lead compensator is developed and simulated in the section 6 for a robotic system. By modelling lead compensator using BGM, the system model from [4] is joined with this compensator in same domain and analysis is performed in section 7.

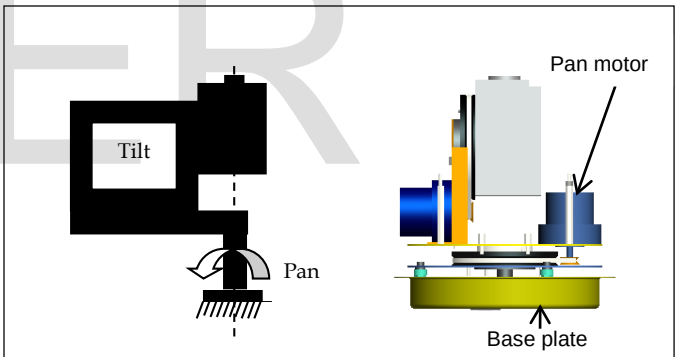

Fig. 2. (a) Schematics and (b) CAD of the pan mechanism

When pan and tilt mechanisms are joined together, they form robotic system with two revolute joints (RR) as in fig 2(b). The applications of these mechanisms working together or independently are object tracking i.e. target acquisition, border patrol, search and rescue etc. The results are summarized in section 8.

The tilt and pan model used in this paper is based on Newton-Euler equation and is discussed in sections 2 and 4. The viscous friction was identified from experiments [14]. The mass and inertia are obtained from CAD as explained in section 2. The tilt mechanism along with lead compensator is analyzed and simulated in Section 3. The pan mechanism along with lead compensator is analyzed and simulated in Section 5. Both the motion controllers are designed to achieve the desired response of the robotic system. The allowable specifications are: the settling time expected to be less than 0.5 seconds; the steady state error can be tolerated within ±2% and the %overshoot is expected to be kept below 5%.

The bond graph model (BGM) of the lead compensator is developed and simulated in the section 6 for a robotic system. By modelling lead compensator using BGM, the system model from [4] is joined with this compensator in same domain and analysis is performed in section 7.

When pan and tilt mechanisms are joined together, they form robotic system with two revolute joints (RR) as in fig 2(b). The applications of these mechanisms working together or independently are object tracking i.e. target acquisition, border patrol, search and rescue etc. The results are summarized in section 8.

2 TILT MECHANISM

The dynamical model of the tilt mechanism is developed in the 2.1. The stability analysis of the tilt mechanism is presented in the 2.2. The transfer function of the tilt mechanism is calculated in the section 2.3. The tilt mechanism response is discussed in 2.4.

2.1 Linear Model of Tilt Mechanism

The linear model of the tilt mechanism follows from the Newton-Euler with a non rigid body effect. The nonlinear model based on the Newton-Euler equation [1, 3] is as follows.

$$\tau = J_{eff}\ddot{\theta} + f_v\dot{\theta} + f_c sgn(\dot{\theta}) + mgl\sin\theta \quad (1)$$

Here τ = Torque, J_{eff} = Effective inertial load, f_v = Viscous friction, f_c = Coulomb friction, $\theta = Angle\ between\ the\ force\ (mg)\ and\ arm\ length\ (l)$.

The effective inertial load of the system is computed from the following relation [14].

$$J_{eff} = J_L + J_p + n^2 J_a \quad (2)$$

J_a = Actuator inertia, J_p = Pulley inertia, J_L = Load inertia, n = ratio between pulleys diameter.

The nonlinear terms in equation (2) are $sgn(\dot{\theta})$ and $\sin\theta$. These terms with nonlinearity are neglected in the linear model of the system. Thus, the linear model follows from (1) takes the following form

$$\tau = J_{eff}\ddot{\theta} + f_v\dot{\theta} \quad (3)$$

This second-order differential equation can be expressed in state space form by introducing the state variables: $x_1 = \theta, x_2 = \dot{\theta}$, with the derivatives as $\dot{x}_1 = \dot{\theta}$, $\dot{x}_2 = \ddot{\theta}$. Thus the state equations are

$$\dot{x}_1 = x_2 \quad (4)$$
$$\dot{x}_2 = -\frac{f_v}{J_{eff}}x_2 + \frac{u}{J_{eff}} \quad (5)$$

The state space model in vector-matrix form is as follows. [9-14]

$$\dot{x} = \begin{bmatrix} 0 & 1 \\ 0 & -\frac{f_v}{J_{eff}} \end{bmatrix} x + \begin{bmatrix} 0 \\ \frac{1}{J_{eff}} \end{bmatrix} u$$
$$y = [1 \quad 0]x$$

Here

$$x = \begin{bmatrix} x_1 \\ x_2 \end{bmatrix}, \dot{x} = \begin{bmatrix} \dot{x}_1 \\ \dot{x}_2 \end{bmatrix}, u = \tau, A = \begin{bmatrix} 0 & 1 \\ 0 & -\frac{f_v}{J_{eff}} \end{bmatrix}, B = \begin{bmatrix} 0 \\ \frac{1}{J_{eff}} \end{bmatrix},$$
$$C = [1 \quad 0] \quad (6)$$

The state space model of the tilt mechanism is described by (6). Now we analyze the stability of the tilt mechanism in 2.2.

2.2 Stability Analysis of Tilt Mechanism

The stability analysis of the tilt mechanism based on its equilibrium points is performed in this section. For the above state space equation (4-5) of the tilt mechanism, we have found all the equilibrium points by putting $u = 0, \dot{x}_1 = 0$ and $\dot{x}_2 = 0$ as follows [2]

$$0 = x_2$$
$$0 = -\frac{f_v}{J_{eff}}x_2$$

The equilibrium points are located at the $(x_1, 0)$ where x_1 belongs to the set of real numbers. The function *f(x)* for the stability analysis of the tilt mechanism follows from (4-5). The type of each isolated equilibrium point can be found using the following function

$$f(x) = \begin{bmatrix} \dot{x}_1 \\ \dot{x}_2 \end{bmatrix} = \begin{bmatrix} x_2 \\ -\frac{f_v}{J_{eff}}x_2 \end{bmatrix} \quad (7)$$

The behavior of the tilt mechanism can be analyzed using (7). The Jacobian of the tilt mechanism given below follows from (7).

$$\frac{\partial f}{\partial x} = \begin{bmatrix} 0 & 1 \\ 0 & -\frac{f_v}{J_{eff}} \end{bmatrix}$$

The Jacobian of the tilt mechanism evaluated at $(x_1, 0)$ is given below

$$A = \frac{\partial f}{\partial x}\Big|_{(x_1,0)} = \begin{bmatrix} 0 & 1 \\ 0 & -\frac{f_v}{J_{eff}} \end{bmatrix}$$

The numerical simulation of stability analysis is performed. Here term $\frac{f_v}{J_{eff}}$ is always greater than 0 (non-negative) and eigenvalues of the A lies at 0 and $-\frac{f_v}{J_{eff}}$. This implies that tilt mechanism is marginally stable.

The viscous friction f_v used in the above expression was determined experimentally. The value of viscous friction is 0.0019 Nms/rad. To find the effective inertial loads of tilt system, the inertial load of the tilt mechanism was analyzed in the Pro-E, the pulley inertia was determined separately in Pro-E and the actuator inertia was obtained from the motor datasheet. The effective load of the tilt mechanism is calculated by using equation (2), and is summarized in table I.

TABLE I

INERTIAL LOAD FOR TILT MECHANISM

	J_L $(Kg\,m^2)$	J_p $(Kg\,m^2)$	J_a $(Kg\,m^2)$	n	J_{eff} $(Kg\,m^2)$
Tilt mechanism	0.0056	4.4×10^{-7}	1.6×10^{-6}	5.7143	0.005653

Thus the Jacobian matrix determined carefully through experimental investigation is given below

$$A = \begin{bmatrix} 0 & 1 \\ 0 & -0.3361 \end{bmatrix}$$

The eigenvalues corresponding to the Jacobian determined were found as follows

$$|\lambda I - A| = \begin{vmatrix} \lambda & -1 \\ 0 & \lambda + 0.3361 \end{vmatrix} = \lambda^2 + 0.3361\lambda = 0$$

$$\lambda_1 = -0.3361, \lambda_2 = 0$$

Thus for the equilibrium points, the eigenvalues are at 0 and -0.8933. As one of the eigenvalues of A is zero, the phase portrait is in some sense degenerated [2]. Here the matrix A has a nontrivial null space. All the vectors in the null space of A are equilibrium points for the system. All the trajectories coverage to the equilibrium subspace as $\lambda_1 < 0$.

2.3 Transfer Function of Tilt Mechanism

The transfer function of the tilt mechanism is found using (6), value of f_v, table I and $G(s) = C(sI - A)^{-1}B$ from [9], and is given below

$$G(s) = \frac{176.8972}{s^2+0.3361s} \quad (8)$$

The tilt mechanism is marginally stable as one of the system poles lies at the origin. The transfer function of the tilt mechanism is described by (8).

2.4 Gain Compensated Tilt Mechanism Response

As noticed in [7,14], the (8) has a settling time, peak time, rise time, percentage overshoot and steady-state error are 24.7 sec, 18.3 sec, 8.7 sec, 4.86 and 2×10^{-3} when the gain (3.3216×10^{-4}) is selected on the root locus with radial line. All the time constants far exceed than desired performance values. This problem has to be compensated by designing the control system, as explained in the next section.

3 MOTION CONTROL OF TILT MECHANISM

The linear tilt system is controlled by lead compensator as shown in fig. 3. The compensated tilt mechanism (tilt mechanism with lead compensator) analysis and simulation via the root locus method is described below.

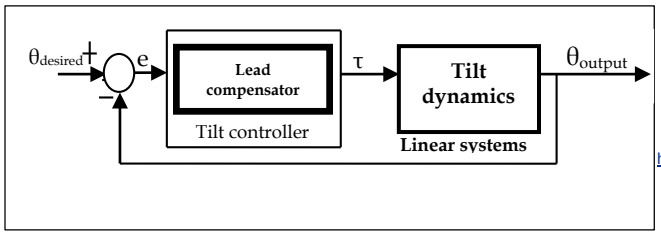

Fig. 3. Tilt feedback control system

The objective of a lead compensator is to drive the T_s to less than 0.5 sec for the unity feedback system shown in fig. 3. The compensated system is schematically shown in fig. 4.

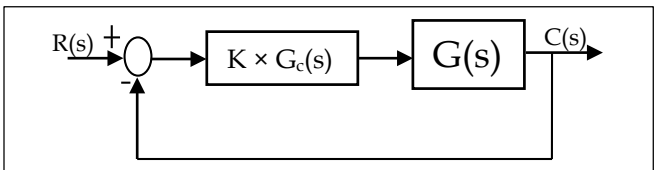

Fig. 4. Closed loop system with compensator

The lead compensator is found by using [9-12]. For the lead compensator, the calculated natural frequency, the desired dominant pole location (DPL) and zero location (z_c) are

$$w_n = 28.9810\ rad/sec, DPL = -20.0000 + 20.9738i,$$
$$Angle\ at\ desired\ pole = \ 93.2076°, z_c = 0.01,$$
$$Anglar\ Contribution\ by\ zero = \ -46.8605°$$

Hence, the compensator angle contribution is 46.57° and thus the lead compensator transfer function may be written as

$$G_c(s) = \frac{s + 0.01}{s+39.6541} \quad (9)$$

The open-loop transfer function resulting for fig. 4 is determined using (8) and (9), and is given below

$$KG(s)G_c(s) = K\frac{176.8972(s + 0.01)}{s(s+0.3361)(s+39.6541)} \quad (10)$$

The open loop transfer function of tilt mechanism with lead compensator was determined in (10). According to the root locus technique [9], it has three branches of root locus, symmetrical with respect to the real axis, real-axis segment are [0,-.01] and [-0.3361,-39.6541], starting points are the open-loop poles at 0, -0.3361 and -39.6541, ending points are the open-loop zeros at -0.01, ∞ (infinity),-∞, real-axis intercept is at -19.9951, angle of asymptotes are 90°, 270° and breakaway point is at -19.9951. The result of root-locus method, based on simulation performed in Matlab is shown in fig. 5 (a).

A damping ratio of 0.69 is represented by a radial line drawn on the root-locus in fig 5(a). We have found dominant pair of poles at $-19.9771 \pm 20.9316i$ along the damping ratio line for a gain (K) equal to 4.6626. The compensated system step response is shown in fig. 5 (b). The closed loop transfer function (T(s)) based on (10) is as follows

$$T(s) = \frac{824.8\,s + 8.248}{s^3 + 39.99\,s^2 + 838.1\,s + 8.248} \quad (11)$$

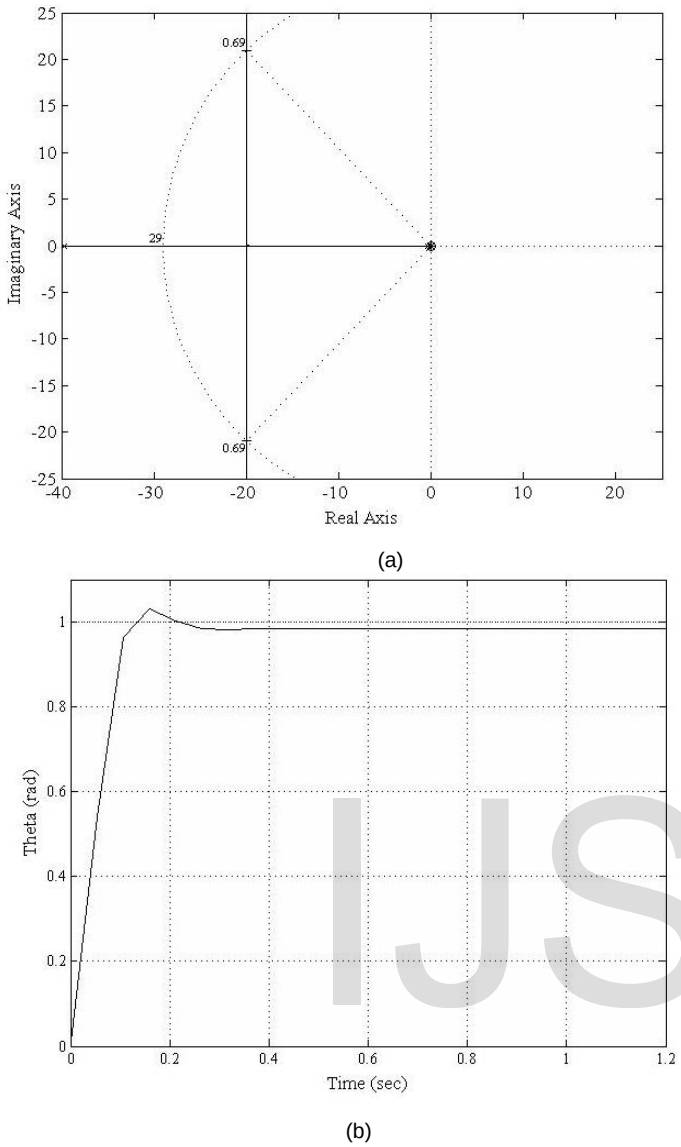

Fig. 5. Compensated system (a) Root locus with radial line (b) step response

As noticed in fig. 5(b), settling time, peak time, rise time, percentage overshoot and steady-state error are equal to 0.18 sec, 0.159 sec, 0.0879 sec, 3.24 and 1.574×10^{-2} respectively. They meet the desired performance values.

4 Pan Mechanism

The dynamical model of the pan mechanism is developed in the 4.1. The stability analysis based on the state space model of the pan mechanism is presented in the 4.2. The transfer function of the pan mechanism is calculated in the 4.3. The pan mechanism response is discussed in 4.4.

4.1 Linear Model of Pan Mechanism

The linear model of the pan mechanism follows from the Newton-Euler equation [1] under certain assumptions. The nonlinear model based on the Newton-Euler equation is as follows.

$$\tau = J_{eff}\ddot{\theta} + f_v\dot{\theta} + f_c sgn(\dot{\theta}) + mgl\sin\theta \quad (12)$$

$$\theta = Angle\ between\ the\ force(mg) and\ arm\ length\ (l)$$

The nonlinear model of pan mechanism presented in [2, 14] can also be used for analysis and simulation. For the pan mechanism $mglsin\theta$ term is effectively equal to zero explained by fig. 2. Therefore, (12) becomes

$$\tau = J_{eff}\ddot{\theta} + f_v\dot{\theta} + f_c sgn(\dot{\theta}) \quad (13)$$

This equation is for the pan mechanism and represents the nonlinear model of pan mechanism. This nonlinear equation needs to be linearized in order to develop a controller for the pan mechanism. The nonlinear term in equation (13) is $sgn(\dot{\theta})$. Therefore, term with nonlinearity is neglected in the linear model of the system. Linearization simplifies the pan model. Thus, the linear model takes the following form

$$\tau = J_{eff}\ddot{\theta} + f_v\dot{\theta} \quad (14)$$

The viscous friction has been determined experimentally. Similar to [7,14], the value of the viscous friction is 0.007 Nms/rad for the pan mechanism. The effective load is calculated by using equation (2), and is shown in table II.

TABLE II
INERTIAL LOAD FOR PAN MECHANISM

	J_L $(Kg\ m^2)$	J_p $(Kg\ m^2)$	J_a $(Kg\ m^2)$	n	J_{eff} $(Kg\ m^2)$
Pan mechanism	0.0743	4.4×10^{-7}	1.6×10^{-6}	5.7143	0.07435

The state space model for pan mechanism was developed as in the case of tilt mechanism and is given below in vector-matrix form.

$$\dot{x} = \begin{bmatrix} 0 & 1 \\ 0 & -\frac{f_v}{J_{eff}} \end{bmatrix} x + \begin{bmatrix} 0 \\ \frac{1}{J_{eff}} \end{bmatrix} u \quad (15)$$
$$y = [1 \quad 0]x$$

In the next section, we have analyzed the stability of the pan mechanism.

4.2 Stability Analysis of Pan Mechanism

The stability analysis of the pan mechanism is based on its equilibrium points. For this purpose, we have found all the equilibrium points similar to section 2.2. The equilibrium points are located at the $(x_1, 0)$ where x_1 belongs to the set of real numbers. Now we analyze the behavior of the pan mechanism at equilibrium points. Similar to (7), the function for the stability analysis of the pan mechanism based on (15) is presented here

$$f(x) = \begin{bmatrix} \dot{x}_1 \\ \dot{x}_2 \end{bmatrix} = \begin{bmatrix} x_2 \\ -\frac{f_v}{J_{eff}} x_2 \end{bmatrix}$$

The Jacobian at $(x_1, 0)$ of the pan mechanism is as follows

$$A = \frac{\partial f}{\partial x}\Big|_{(x_1,0)} = \begin{bmatrix} 0 & 1 \\ 0 & -\frac{f_v}{J_{eff}} \end{bmatrix}$$

Using the values of f_v (0.007) and J_{eff}(0.07435) the expression above takes the following form

$$A = \begin{bmatrix} 0 & 1 \\ 0 & -0.09415 \end{bmatrix}$$

The eigenvalues are found as

$$|\lambda I - A| = \begin{vmatrix} \lambda & -1 \\ 0 & \lambda + 0.09415 \end{vmatrix} = \lambda^2 + 0.09415\lambda = 0$$

$$\lambda_1 = -0.09415, \lambda_2 = 0$$

For the equilibrium points at (x_1,0) the eigenvalues are at 0 and -0.09415. As one of the eigenvalues of A is zero, the phase portrait is in some sense degenerated. Therefore, matrix A has a nontrivial null space. All vectors in the null space of A are equilibrium points for the system. All the trajectories converge to the equilibrium subspace as $\lambda_1 < 0$.

4.3 Transfer Function of Pan Mechanism

The transfer function of the pan mechanism is determined using (15), value of f_v, table II and $G(s) = C(sI - A)^{-1}B$, and is given below

$$G(s) = \frac{13.4499}{s^2 + 0.09415s} \quad (16)$$

4.4 Gain Compensated Pan Mechanism Response

Similarly, as noticed in [7,14], for (16) the settling time, rise time, peak time, percentage overshoot and steady-state error are 87.8 sec, 30.7 sec, 63 sec, 5.05 and 2×10^{-3} respectively, when the gain (3.4719×10^{-4}) is selected on the intersection of the root locus and the radial line for a unity feedback system with gain K. These values far exceed the desired performance values. This deficiency has to be compensated by designing the control system. The design of control system for the pan mechanism is explained in the next section.

5 Motion Control of Pan Mechanism

The linear pan mechanism is controlled by lead compensator to meet the desired conditions on the transient and the steady state response as shown in fig. 6. The compensated pan system (pan mechanism with lead compensator) analysis and simulation via the root locus method is presented here.

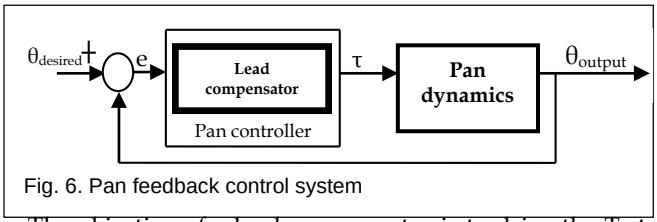

Fig. 6. Pan feedback control system

The objective of a lead compensator is to drive the Ts to less than 0.5 sec for the unity feedback system. The compensated system is schematically shown in fig. 6. The lead compensator is found by using [9-12]. For the lead compensator, the calculated natural frequency, the desired dominant pole location (DPL) and zero location (zc) are

$w_n = 28.9855\ rad/sec,\ \ DPL = -20.00 + 20.9739\ i,$
Angle at desired pole = $92.2711^{\circ}, z_c = 0.01,$
Anglar Contribution by zero = -46.3471°

Hence, the compensator angle contribution is 46.3818° and thus the lead compensator is

$$G_c(s) = \frac{s + 0.01}{s + 39.99} \quad (17)$$

The open-loop transfer function resulting for fig. 6 is determined by using (16) and (17), and is given below

$$KG(s)G_c(s) = K\frac{13.4499(s + 0.01)}{s(s + 0.09415)(s + 39.99)} \quad (18)$$

The transfer function of pan system with lead compensator was determined in (18). According to the root locus technique [9], it has three branches of root locus, symmetrical with respect to the real axis, real-axis segment is [0,-0.01] and [-0.09415,-39.99], starting points are the open-loop poles at 0, -0.09415 and -39.99, ending points are the open-loop zeros at -0.01, ∞ (infinity),-∞, real-axis intercept is at -20.0421, angle of asymptotes are 90°, 270°, breakaway point is at -20.0421. The result of the root-locus method, based on simulation performed using Matlab is shown in fig. 7 (a) and (b).

A damping ratio of 0.69 is represented by a radial line intersecting the root-locus. We have found dominant pair of poles at $-19.8993 \pm 20.8851i$ along the damping ratio line for a gain (K) equal to 61.4550. The compensated system step response is shown in fig. 7 (b). The closed loop transfer function T(s) based on (18) is as follows.

$$T(s) = \frac{830.3\ s + 8.266}{s^3 + 39.69\ s^2 + 830.3\ s + 8.266} \quad (19)$$

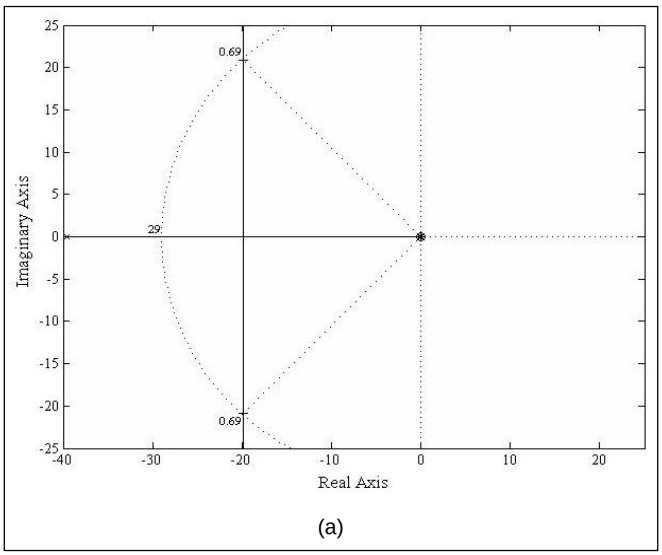

(a)

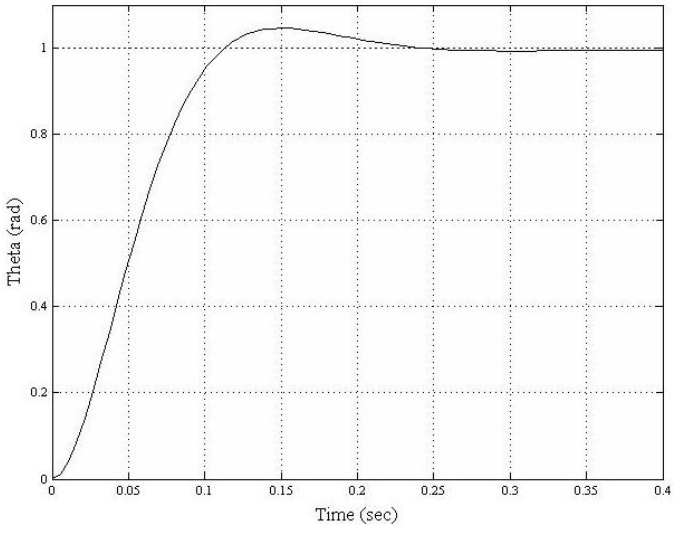

(b)

Fig. 7. Compensated pan system (a) root locus with radial line (b) step response

As noticed in fig. 7(b), the settling time, rise time, peak time, percentage overshoot and the steady-state error are equal to 0.202 sec, 0.0733 sec, 0.15 sec, 4.63 and 6×10^{-3} respectively. They meet the desired performance values.

6 Bond Graph model of Lead Compensator

The lead compensator circuit is implementable using the passive components such as resistor and capacitor as shown in the fig. 8.

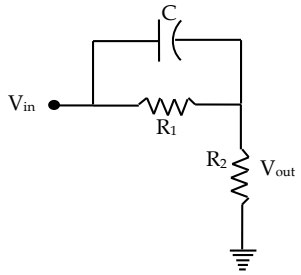

Fig. 8. Lead compensator

In fig. 8, the C, R_1, R_2, V_{in} and V_{out} represent the capacitor, resistor 1, resistor 2, input voltage and output voltage respectively. The values of these components are found by equating the following equation with the transfer function of lead compensator in section 3 and 5.

$$G(s) = \frac{V_{out}}{V_{in}} = \frac{{}^{1}/_{R_1}+Cs}{{}^{1}/_{R_1}+{}^{1}/_{R_2}+Cs} \quad (20)$$

The values found by using (20) are used in the bond graph model of lead compensator. The equivalent bond graph model of the lead compensator is shown in fig. 9.

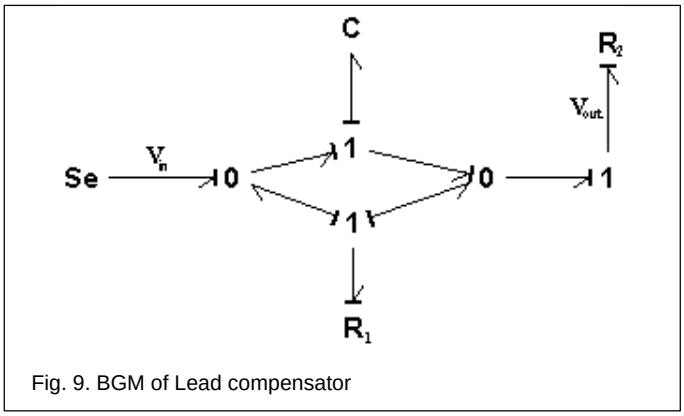

Fig. 9. BGM of Lead compensator

Here Se represents the source of effort. The 0 and 1-junctions are the representation of KCL and KVL in bond graph modeling respectively. The controller such as lead compensator is modeled using BGM here. Similarly, the lag, lag-lead compensators can be modeled.

7 BGM of a System and Controller

The BGM of robotic system [4] such as a tilt mechanism, and a pan mechanism with BGM of lead compensator has added new dimension in this research work. The system has been already modeled using BGM [4] and now a lead compensator has been modeled using BGM. This research work leads to system and controller modelling using BGM technique as shown in fig. 10. The I_{12} indicates the inertia due to DC motor and I_{18} indicates the inertia due to load attached with pulley 2. The R_{11} indicates the viscous friction due to DC motor and R_{15} indicates the viscous friction between the pulleys and R_{19} indicates the viscous friction due to load. The TF indicates the gear ratio.

The reduced bond graph model of the robotic system with lead compensator is shown in fig. 11. Each storage element in the BGM contributes the state that will appear in the state space model. From the fig. 11, it is concluded that BGM of robotic system with lead compensator contributes the 3 states and hence the order of the characteristic equation is 3.

In the close loop, the BGM of robotic system with lead compensator is presented in fig. 12. The results of BGM match with the results of section 3 and 5.

The BGM of robotic system gives the information that state space model is controllable and observable as presented in fig. 10. In fig 10, BGM of robotic system indicates that both the storage elements have integral causality and inverse BGM of robotic system indicates that 2 storage elements have differential causality. Therefore, the order of denumerator is 2 in the transfer function of robotic system.

The state space model is obtained directly from the BGM. The numerical analysis of controllability and observability matrices for the considered system indicate that it is controllable and observable.

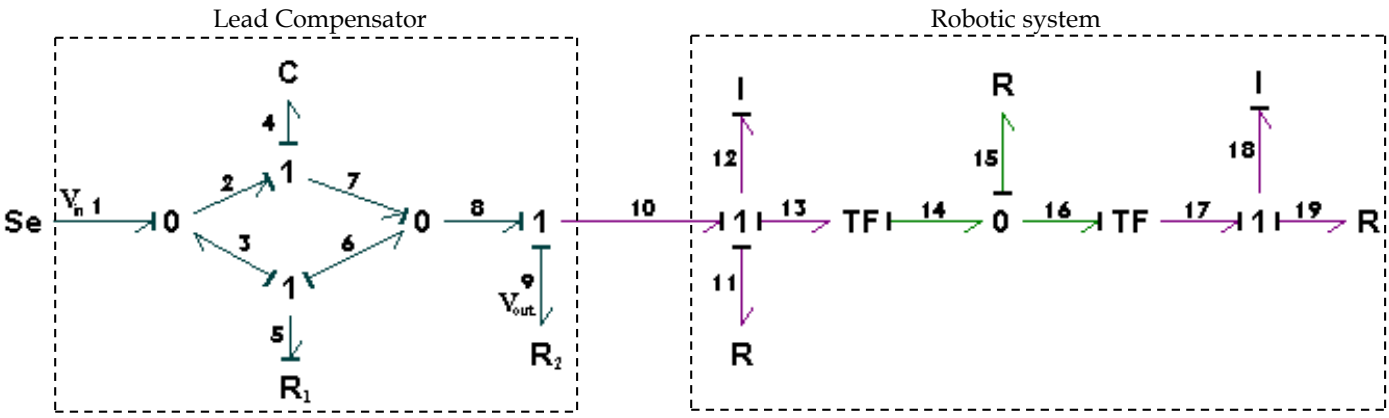

Fig. 10. BGM of robotic system with Lead compensator

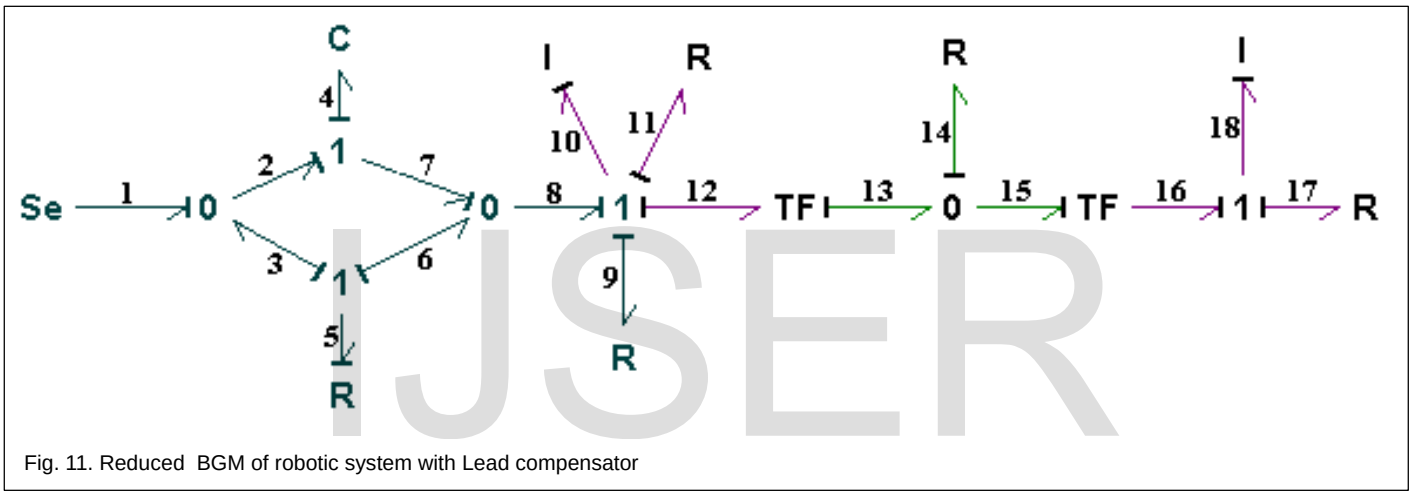

Fig. 11. Reduced BGM of robotic system with Lead compensator

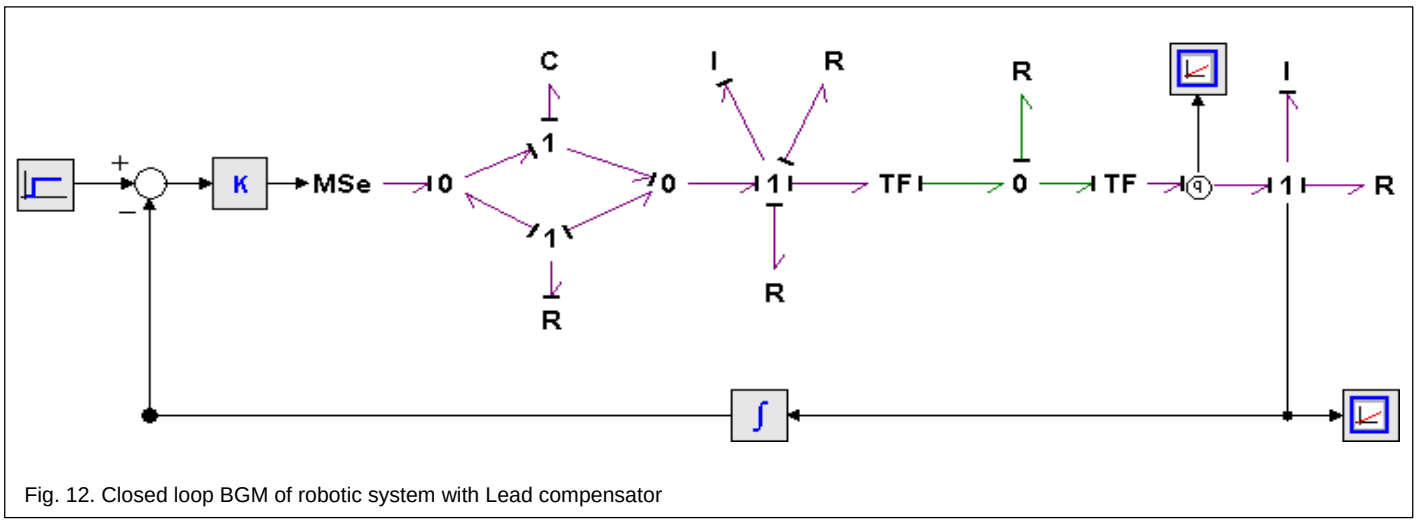

Fig. 12. Closed loop BGM of robotic system with Lead compensator

This proves that bond graph can be used as an effective modelling method for the systems and controllers. By using the

Newton-Euler method, the equation formed has equivalent effects. By using the BGM, all the component of mechatronics system such as robotic system considered are exactly modeled without taking the equivalent effect in [4].

8 RESULTS

Linear modelling of the tilt and pan mechanisms and its motion control based on feedback control system using the lead compensators for them leads to the desired results presented in the table III.

TABLE III
COMPENSATED SYSTEM MODEL RESULTS

	T_S (seconds)	e_{SS}	%OS
Tilt Mechanism	0.159	1.574×10^{-2}	3.24
Pan Mechanism	0.202	6.000×10^{-3}	4.63

- The values of settling time meet the desired performance value for both mechanisms. The desired performance value is set according to the settling time of the eye ball.
- The percentage overshoots and steady state errors are within desired performance values.

In order that the steady state error and %OS do not increase more than the desired values, encoder and Optoschmitt sensor are used in the real time system. The Optoschmitt sensor checks that %OS does not increase more than the desired value. The encoder attached with motor gives the position of motor shaft. The positioning accuracy of 0.0015 rad was achieved for the pan and tilt mechanisms. This was achieved by using the DC-motor having encoder of resolution 4096 pulses/revolution. This ensures the steady state error stays below the desired value (<2%).

The model of the pan and tilt mechanisms with lead compensators gives us desired orientation of camera. This work is applicable to the mechatronic systems such as robotic arms and serial or parallel linked robotic mechanisms. Thus robotics system is appropriate for tracking systems. The lead compensator has been modeled using the bond graph modeling which added a novelty in this research work. Thus systems such as pan and tilt mechanisms and controllers such as lead compensators, both are modeled using bond graph modeling technique. This has reduced requirement of the factors such as modulated source of effort "MSe" to join the two different domains such as MSe [16] has been used in the [4] to join the controller with tilt mechanism. The results obtained from the conventional technique presented in section 3 to 5 matched closely with the results of section 7.

ACKNOWLEDGMENTS

The authors are indebted to the Air University, Islamabad the Higher Education Commission of Pakistan for having made this research work possible.

REFERENCES

[1] Schilling R.J., "Fundamental of robotics analysis and control", Prentice Hall, India, pp 170-177, 1990.
[2] Khalil H.K., "Nonlinear system", Prentice Hall, USA, 3rd edition, pp. 35 – 60, 2002.
[3] Craig J.J., "Introduction to Robotics Mechanics and Control", Addison-Wesley, 3rd edition, pp. 153, 196-197, 2007.
[4] Sarwar I.S., Malik A.M., Sarwar S.M., "Modelling, Stability Analysis and Dynamic Response of a Multi-Domain Mechatronic System", Proceedings of MATHMOD 2009 - 6th Vienna International Conference on Mathematical Modelling, Austria, pp. 1983-1994, Feb 2009.
[5] Evans W.R., "Control system synthesis by root locus method", AIEE Transactions, vol. 69, pp.547 – 551, 1950.
[6] Pollak C.D., Thaler G.J., "s-plane design of compensators for feedback systems," IRE Trans. Automat. Contr., vol. 6, Sep 1961, pp. 333 - 340.
[7] Sarwar I.S., Malik A.M., "Modelling, analysis and simulation of a Pan Tilt Platform based on linear and nonlinear systems", Proceedings of IEEE/ASME, Mechatronic and Embedded Systems and Applications, China, pp.147–152, Oct 2008.
[8] Gonçalves J.B., Zampieri D.E., "An integrated control for a biped walking robot", Journal of the Brazilian Society of Mechanical Sciences and Engineering, J. Braz. Soc. Mech. Sci. & Eng. vol.28 no.4 Rio de Janeiro, Oct./Dec. 2006.
[9] Nise N.S., "Control systems engineering", Wiley student edition, Forth edition, India, pp. 515-524, 2004.
[10] Zhang J., Xu S., Li J., "A new design approach of PD controllers", Elsevier, pp. 329–336, Mar 2005.
[11] Monje C.A., Calderón A.J., Vinagre B.M., Feliu, V., "The Fractional Order Lead Compensator", Proceedings of the IEEE International Conference on Computational Cybernetics, Vienna, Austria, pp.347–352, 2004.
[12] Messner W., "The development, properties, and application of the complex phase lead compensator", Proceedings of the American Control Conference Chicago, Illinois, IEEE, Jun 2000.
[13] Sarwar I.S., "Design, modelling and control of Pan Tilt Platform for unmanned aerial vehicle", M.S. thesis, Dept. Mechatronics Eng., NUST, Rawalpindi, Pakistan, 2006.
[14] Sarwar I.S., Malik A.M., "Analysis and simulation of a Pan Tilt Platform based on linear model", NUST Journal of Engineering Sciences, Vol. 1, No. 1, Dec 2008, pp.12–17.
[15] Ogata K., "Modern Control Engineering", Prentice Hall, USA, 5th edition, pp. 409 – 417, 2010.
[16] Controllab products B.V.: 20 Sim the power in modelling. The Netherlands.